Digital Signal Processing 33 (2014) 42–49

Contents lists available at ScienceDirect

Digital Signal Processing

www.elsevier.com/locate/dsp

Channel equalization for synchronization of chaotic maps

Renato Candido, Marcio Eisencraft, Magno T.M. Silva *

Escola Politécnica, Universidade de São Paulo, São Paulo, 05508-010, Brazil

ARTICLE INFO

Article history:
Available online 11 July 2014

Keywords:
Synchronization of chaotic maps
Chaos-based communication
Adaptive equalization
Non-ideal channels

ABSTRACT

Many communication systems applying synchronism of chaotic systems have been proposed as an alternative spread spectrum modulation that improves the level of privacy in data transmission. However, due to the lack of robustness of chaos synchronization, even minor channel imperfections are enough to hinder communication. In this paper, we propose an adaptive equalization scheme based on a modified normalized least-mean-squares (NLMS) algorithm, which enables chaotic synchronization when the communication channel is not ideal. As an example of application, this scheme is used to recover a binary sequence modulated by a chaotic signal generated by the Hénon map. Simulation results show that the modified NLMS can successfully equalize the channel in different scenarios.

1. Introduction

In the last two decades, the feasibility of communication systems based on the synchronism of chaotic systems has been theoretically and experimentally investigated (e.g., [1–5]). Chaotic signals are deterministic, aperiodic, limited, and present sensitive dependence on initial conditions [6]. Therefore, they have been proposed as broadband information carriers and may yield interesting properties like multipath and jamming immunity [7–9]. Besides, they have the potential of providing high level of privacy in data transmission [4,10].

Recently, some works with a practical approach using chaotic synchronization have appeared, mainly in the optical communication domain (see, e.g., [4,11]). This is somewhat natural since chaotic generators can be easily created using the intrinsic nonlinear properties of lasers [11]. This fact was exploited in [4], where a high-speed long-distance communication system based on chaos synchronization was demonstrated over a commercial fibre-optic link. In this system, it was possible to obtain bit error ratios next to the usually expected in a conventional communication system. However, it is important to notice that the dispersion effects were compensated in a non-adaptive manner. The system as proposed in [4] would perform badly in a wireless channel where distortions vary constantly in time due to multipath, changing noise sources, and other time-variant impairments.

In fact, one of the worst drawbacks in chaos-based communication systems is the lack of robustness of chaotic synchronization with respect to noise and intersymbol interference (ISI) introduced by the channel. Even minor noise levels or simple linear distortions are enough to hinder communication, which usually depends on identical synchronization [12,13]. Many chaos-based communication systems, if implemented as proposed in the literature, tend to present prohibitive bit error rates in non-ideal channels when compared to their conventional counterparts [13]. Although some preliminar results were obtained in more realistic channels [5,14,15], it is of paramount importance to propose schemes that can adapt to the practical impairments of real communication channels. Otherwise they have no chance of being of commercial interest.

In conventional communication systems, it is usual to consider an equalizer in the receiver to mitigate the ISI introduced by the channel [16–18]. Equalization schemes applied to chaotic synchronization have been proposed in the literature for different approaches of message encoding (see, e.g., [19–24] and their references). To the best of our knowledge, only [24] considers the equalization in the discrete-time domain applied to a Wu and Chua's chaotic synchronization scheme, in which an encoded message is fed back into the chaotic signal generator (CSG). The main drawback of the scheme of [24] is that it uses the Ikeda map to encode the message and the encoded signal may not be chaotic. This occurs because the Ikeda map presents a stable fixed point besides the chaotic attractor [6].

In this paper, we propose an adaptive equalizer for a chaotic synchronization scheme in a master–slave configuration using the Hénon map, which ensures that the transmitted signal is in fact chaotic, as we shall see. As in [24], the chaotic synchronization scheme considered here feeds back the encoded message into the

* Corresponding author.
E-mail addresses: renatocan@lps.usp.br (R. Candido), marcio@lcs.poli.usp.br (M. Eisencraft), magno@lps.usp.br (M.T.M. Silva).

http://dx.doi.org/10.1016/j.dsp.2014.07.001
1051-2004/

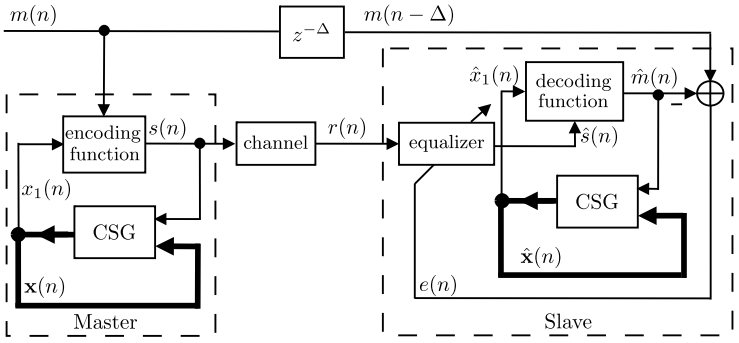

Fig. 1. Chaotic synchronization system with an adaptive equalizer.

CSG. As this situation is a discrete-time model for the practical set described in [4], we consider it as a relevant scenario.

The paper is organized as follows. In Section 2, we describe a discrete-time version of the Wu and Chua's chaotic synchronization [3,10], which besides a noisy and dispersive channel includes an adaptive equalizer. In Section 3, we modify the normalized least-mean-squares (NLMS) algorithm to take into account the Hénon map. The interval of the step-size to ensure a local and weak stability of the proposed algorithm is obtained in Section 4. Section 5 presents simulation results of a communication system based on this scheme and, in Section 6, we draft the conclusions. Although we consider the Hénon map in this paper, our scheme can be straightforwardly extended to other chaotic maps.

2. Problem formulation

Fig. 1 shows the chaotic synchronization problem under consideration. It is based in a discrete-time version of the one proposed in [3]. In our scheme, a binary signal $m(n) \in \{-1, +1\}$ is encoded by using the first component of the master state vector $\mathbf{x}(n)$, via a coding function

$$s(n) = c\big(x_1(n), m(n)\big), \tag{1}$$

so that $m(n)$ can be recovered using the inverse function with respect to $m(n)$, i.e.,

$$m(n) = c^{-1}\big(x_1(n), s(n)\big). \tag{2}$$

Then, the signal $s(n)$ is fed back into the chaotic signal generator (CSG) and transmitted through a communication channel, whose model is constituted by a transfer function $H(z)$ and additive white Gaussian noise (AWGN). We assume an M-tap adaptive equalizer, with input regressor vector

$$\mathbf{r}(n) = \begin{bmatrix} r(n) & r(n-1) & \cdots & r(n-M+1) \end{bmatrix}^T$$

and output

$$\hat{s}(n) = \mathbf{r}^T(n)\mathbf{w}(n-1),$$

where $(\cdot)^T$ indicates transposition and

$$\mathbf{w}(n-1) = \begin{bmatrix} w_0(n-1) & w_1(n-1) & \cdots & w_{M-1}(n-1) \end{bmatrix}^T$$

is the equalizer weight vector. The equalizer must mitigate the intersymbol interference introduced by the channel and recover the encoded signal $s(n)$ with an unavoidable delay of Δ samples.

If transmitter and receiver identically synchronize [25], i.e., if $\hat{\mathbf{x}}(n) \to \mathbf{x}(n)$, then using the output of the equalizer and the estimate of $x_1(n)$, $m(n)$ can be decoded via

$$\hat{m}(n) \triangleq c^{-1}\big(\hat{x}_1(n), \hat{s}(n)\big) \to m(n), \tag{3}$$

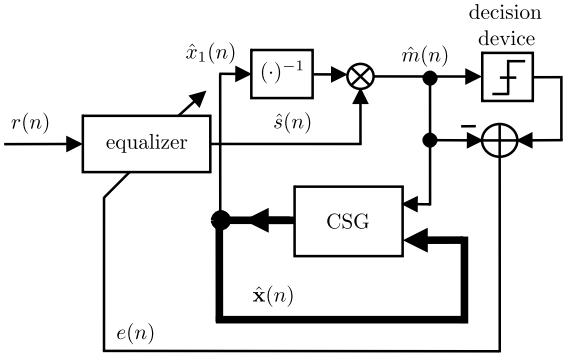

Fig. 2. Receiver of the chaotic communication system with an adaptive equalizer in the decision-directed mode.

where $\hat{x}_1(n)$ is the first component of the slave state vector $\hat{\mathbf{x}}(n)$. Thus, the estimation error

$$e(n) = m(n-\Delta) - \hat{m}(n) \tag{4}$$

can be used as an equalization criterion. Once identical master–slave synchronization is obtained, $m(n)$ can be used to transmit information between the two systems, being $\hat{m}(n)$ the decoded binary message.

We are assuming that there is a training sequence $\{m(n-\Delta)\}$, known in advance at the receiver. In this case, the equalizer works in the *training mode* and updates its coefficients in a supervised manner, using the estimation error in conjunction with an adaptive algorithm. If we intend to transmit information using $m(n)$, the receiver will not have access to $\{m(n-\Delta)\}$ and this sequence will be replaced by the output of the decision device, as shown in Fig. 2. In this case, the equalizer works in the so-called *decision-directed mode*. Due to variations in the communication channel, the switching between these two modes must occur whenever the mean-squared error achieves a predefined threshold [16–18]. Although this switching occurs in the practice, we only consider the *training mode* in the simulations of Section 5.

In this paper, the Hénon map [26] is used in both CSGs of Fig. 1. Therefore, the equations governing the global dynamical system can be written as

$$\mathbf{x}(n+1) = \mathbf{A}\mathbf{x}(n) + \mathbf{b} + \mathbf{f}\big(s(n)\big), \tag{5}$$

$$\hat{\mathbf{x}}(n+1) = \mathbf{A}\hat{\mathbf{x}}(n) + \mathbf{b} + \mathbf{f}\big(\hat{s}(n)\big), \tag{6}$$

where $\mathbf{x}(n) \triangleq [x_1(n)\ x_2(n)]^T$, $\hat{\mathbf{x}}(n) \triangleq [\hat{x}_1(n)\ \hat{x}_2(n)]^T$,

$$\mathbf{A} = \begin{bmatrix} 0 & \beta \\ 1 & 0 \end{bmatrix}, \qquad \mathbf{b} = \begin{bmatrix} \alpha \\ 0 \end{bmatrix}, \qquad \mathbf{f}\big(s(n)\big) = \begin{bmatrix} -s^2(n) \\ 0 \end{bmatrix}, \tag{7}$$

being β and α real constant parameters of the map.

In [27] it was shown that, under ideal channel conditions, i.e., when $r(n) \equiv s(n)$ and the equalizer is an identity system, identical synchronization between master and slave is obtained if all the eigenvalues of $\mathbf{A}$ are inside the unit circle. Since the eigenvalues of $\mathbf{A}$ are $\pm\sqrt{\beta}$, we conclude that for $|\beta| < 1$, master and slave identically synchronize under ideal conditions. Therefore, from (3), $\hat{m}(n) \to m(n)$.

As coding function, we consider [10,24]

$$s(n) = c\big(x_1(n), m(n)\big) = x_1(n) \cdot m(n) \tag{8}$$

which leads to the decoding

$$\hat{m}(n) = \frac{\hat{s}(n)}{\hat{x}_1(n)}. \tag{9}$$

This particular choice associated to the Hénon map has an interesting property: for a binary polar message ($m(n) = \pm 1$), we can observe from (8) that $s^2(n) = x_1^2(n)$. Thus, (5) does not depend on $m(n)$ and the message does not disturb the Hénon CSGs. This means that, the transmitted signal is in fact chaotic as long as the signals generated by the CSGs are chaotic. For instance, this is not the case in [24], where the Ikeda map was used or in [27], where an additive coding function was employed instead of the multiplicative one as that of (8).

3. The chaotic NLMS algorithm

Stochastic-gradient algorithms update the coefficients of an adaptive equalizer using the following equation

$$\mathbf{w}(n) = \mathbf{w}(n-1) - \rho \nabla_{\mathbf{w}} \hat{J}(n), \tag{10}$$

where ρ is a step size and $\nabla_{\mathbf{w}} \hat{J}(n)$ is the gradient vector of the instantaneous cost-function $\hat{J}(n)$ to be minimized. Using (10), the coefficient vector $\mathbf{w}(n-1)$ is updated in the direction opposite to that of the gradient of $\hat{J}(n)$, which in turn is a function of the estimation error. Different functions lead to algorithms with different properties as convergence rate, computational cost, tracking capability, among others [17,18]. The squared error is the cost-function most used in the literature and leads to the popular LMS algorithm.

In order to obtain a version of the LMS algorithm to adapt the equalizer in the scheme of Fig. 1, we begin by defining the following instantaneous cost-function

$$\hat{J}(n) = e^2(n) = \big[m(n-\Delta) - \hat{m}(n)\big]^2. \tag{11}$$

Computing the gradient of $\hat{J}(n)$ with respect to the coefficient vector $\mathbf{w}(n-1)$, we obtain

$$\nabla_{\mathbf{w}} \hat{J}(n) = 2e(n)\frac{\partial e(n)}{\partial \mathbf{w}(n-1)} = -2e(n)\frac{\partial \hat{m}(n)}{\partial \mathbf{w}(n-1)}. \tag{12}$$

Assuming that $\hat{x}_1(n) \neq 0$ for all n and taking into account the equalizer in the scheme of Fig. 1, (3) can be rewritten as

$$\hat{m}(n) = \frac{\hat{s}(n)}{\hat{x}_1(n)} = \frac{\mathbf{r}^T(n)\mathbf{w}(n-1)}{\hat{x}_1(n)}. \tag{13}$$

Using (13) and assuming that $\hat{x}_1(n)$ does not depend on $\mathbf{w}(n-1)$, we arrive at

$$\nabla_{\mathbf{w}} \hat{J}(n) = -2\frac{e(n)}{\hat{x}_1(n)}\frac{\partial \hat{s}(n)}{\partial \mathbf{w}(n-1)} = -2\frac{e(n)}{\hat{x}_1(n)}\mathbf{r}(n). \tag{14}$$

Thus, replacing (14) in (10) and considering $\rho = \mu$ as step size, we arrive at the update equation of the chaotic[1] LMS (cLMS) algorithm, given by

$$\mathbf{w}(n) = \mathbf{w}(n-1) + \mu\frac{e(n)}{\hat{x}_1(n)}\mathbf{r}(n). \tag{15}$$

It is well known in the adaptive filtering literature that one problem with the LMS algorithm is how to choose the step-size μ to enable a high convergence rate, provide an acceptable steady-state mean-square error, and even ensure its stability [17,18]. Variable step-size algorithms make this choice in a more proper manner and may outperform their non-normalized counterparts, mainly when the statistics of the input signals change quickly. This is the case of the normalized LMS algorithm [17,18]. Therefore, a normalized version of the cLMS algorithm is more adequate to update the coefficients of the equalizer in the scheme of Fig. 1.

To obtain a normalized version of cLMS, we first define the *a posteriori* error as

$$e_p(n) = m(n-\Delta) - \frac{\mathbf{r}^T(n)\mathbf{w}(n)}{\hat{x}_1(n)}. \tag{16}$$

Using (15), $e_p(n)$ can be rewritten as

$$\begin{aligned} e_p(n) &= m(n-\Delta) - \frac{\mathbf{r}^T(n)[\mathbf{w}(n-1) + \mu\frac{e(n)}{\hat{x}_1(n)}\mathbf{r}(n)]}{\hat{x}_1(n)} \\ &= e(n)\left[1 - \mu\frac{\|\mathbf{r}(n)\|^2}{\hat{x}_1^2(n)}\right]. \end{aligned} \tag{17}$$

To enforce $e_p(n) = 0$ at each iteration n, we must select $\mu(n) = \hat{x}_1^2(n)/\|\mathbf{r}(n)\|^2$. Introducing a fixed step-size $\tilde{\mu}$ to control the rate of convergence and a regularization factor δ to prevent division by zero in $\mu(n)$, and replacing the resulting step size in (15), we obtain the update equation of the chaotic NLMS (cNLMS) algorithm, i.e.,

$$\mathbf{w}(n) = \mathbf{w}(n-1) + \frac{\tilde{\mu}}{\delta + \|\mathbf{r}(n)\|^2}\hat{x}_1(n)e(n)\mathbf{r}(n). \tag{18}$$

Note that cNLMS depends not only on the estimation error $e(n)$, but also on $\hat{x}_1(n)$. Since $\hat{x}_1(n)$ depends nonlinearly on $\hat{s}(n-1)$, cNLMS is a nonlinear version of NLMS. Moreover, the synchronization between master and slave in chaotic communication system depends on the mitigation of the intersymbol interference, which is the role played by the equalizer.

We prevent division by a value close to zero in the computation of $\hat{m}(n)$, by making

$$\hat{m}(n) = \operatorname{sign}\big[\hat{s}(n)\hat{x}_1(n)\big]$$

when $|\hat{x}_1(n)| < \varepsilon$, where ε is a small positive constant and

$$\operatorname{sign}[x] = \begin{cases} -1, & x < 0 \\ 1, & x \geq 0 \end{cases}.$$

In order to ensure the stability of the algorithm and to avoid wrong estimates when $\hat{x}_1(n)$ is too large, we introduce a bound for $\hat{x}_1(n)$, i.e., if $|\hat{x}_1(n)| > X$, we simply make $\hat{x}_1(n) \leftarrow X \operatorname{sign}[\hat{x}_1(n)]$, where X is a positive constant. We do not observe performance degradation in different simulation scenarios, when we used $X = 100$. The proposed algorithm is summarized in Table 1.

4. Stability conditions

Using (13), the update equation of cNLMS can be rewritten as

$$\begin{aligned} \mathbf{w}(n) = &\left[\mathbf{I} - \frac{\tilde{\mu}}{\delta + \|\mathbf{r}(n)\|^2}\mathbf{r}(n)\mathbf{r}^T(n)\right]\mathbf{w}(n-1) \\ &+ \tilde{\mu}\hat{x}_1(n)m(n)\frac{\mathbf{r}(n)}{\delta + \|\mathbf{r}(n)\|^2}, \end{aligned} \tag{19}$$

[1] We use the term *chaotic* for the algorithms derived here only for distinguishing them from the original versions of LMS and NLMS algorithms (see, e.g., [18]). The use of this term does not imply a chaotic behavior of the algorithms.

Table 1
Summary of the cNLMS algorithm.

Initialize the algorithm by setting:
$\mathbf{w}(-1) = \mathbf{0}$, $\hat{\mathbf{x}}(0) = [0.1 \ -0.1]^T$
$\mathbf{A} = \begin{bmatrix} 0 & \beta \\ 1 & 0 \end{bmatrix}$, $\mathbf{b} = \begin{bmatrix} \alpha \\ 0 \end{bmatrix}$
α, β: parameters of the Hénon map
δ, ε: small positive constants
X: large positive constant
$0 < \tilde{\mu} < 2$

For $n = 0, 1, 2, 3, \ldots$, compute:
$\hat{s}(n) = \mathbf{r}^T(n)\mathbf{w}(n-1)$
if $|\hat{x}_1(n)| > X$
$\hat{x}_1(n) \leftarrow X \operatorname{sign}[\hat{x}_1(n)]$
end
if $|\hat{x}_1(n)| \leq \varepsilon$
$\hat{m}(n) = \operatorname{sign}[\hat{s}(n)\hat{x}_1(n)]$
else
$\hat{m}(n) = \dfrac{\hat{s}(n)}{\hat{x}_1(n)}$
end
$e(n) = m(n-\Delta) - \hat{m}(n)$
$\mathbf{w}(n) = \mathbf{w}(n-1) + \dfrac{\tilde{\mu}}{\delta + \|\mathbf{r}(n)\|^2}\hat{x}_1(n)e(n)\mathbf{r}(n)$
$\hat{\mathbf{x}}(n+1) = \mathbf{A}\hat{\mathbf{x}}(n) + \mathbf{b} + \begin{bmatrix} -\hat{s}^2(n) \\ 0 \end{bmatrix}$
end

where $\mathbf{I}$ is the identity matrix with dimensions $M \times M$. The matrix between brackets has $M-1$ eigenvalues equal to one and one eigenvalue equal to

$$\lambda_1 = 1 - \tilde{\mu}\frac{\mathbf{r}^T(n)\mathbf{r}(n)}{\delta + \|\mathbf{r}(n)\|^2}.$$

Noticing that

$$0 \leq \frac{\mathbf{r}^T(n)\mathbf{r}(n)}{\delta + \|\mathbf{r}(n)\|^2} < 1,$$

and for $\|\mathbf{r}(n)\|^2 \gg \delta$, $\mathbf{r}^T(n)\mathbf{r}(n)/(\delta + \|\mathbf{r}(n)\|^2) \approx 1$, in order to ensure $|\lambda_1| < 1$, we must choose $\tilde{\mu}$ in the interval

$$0 < \tilde{\mu} < 2. \tag{20}$$

The norm of the second term of the r.h.s. of (19) is bounded, i.e.,

$$0 \leq \tilde{\mu}\left|\hat{x}_1(n)\right|\left|m(n)\right|\frac{\|\mathbf{r}(n)\|}{\delta + \|\mathbf{r}(n)\|^2} \leq \tilde{\mu}X\frac{\sqrt{\delta}}{2\delta} < \infty.$$

Therefore, using (deterministic) exponential stability results for the LMS algorithm [28], we conclude that cNLMS is stable in a robust sense if $\tilde{\mu}$ is chosen in the interval (20).

5. Simulation results

In order to verify the behavior of the cNLMS algorithm, we have performed simulations assuming the Hénon map with $\alpha = 1.4$ and $\beta = 0.3$. The state vectors of (5) and (6) were initialized as $\mathbf{x}(0) = \mathbf{0}$ and $\hat{\mathbf{x}}(0) = [0.1 \ -0.1]^T$, respectively. Other initializations also allow equally good results in terms of synchronization when the equalizer mitigates reasonably well the intersymbol interference. Furthermore, the equalizers were initialized as $\mathbf{w}(0) = \mathbf{0}$ and, for comparison, we also consider the system of Fig. 1 without equalizer, in which $\hat{s}(n) = r(n)$.

As performance measure, we consider the excess mean-square error (EMSE) [17,18], defined as

$$\text{EMSE} \triangleq \mathrm{E}\left\{e_a^2(n)\right\}, \tag{21}$$

where $\mathrm{E}\{\cdot\}$ represents the expectation operation,

$$e_a(n) = \mathbf{r}^T(n)\left[\mathbf{w}_o - \mathbf{w}(n-1)\right],$$

and $\mathbf{w}_o$ is the Wiener solution [17,18], computed as

$$\mathbf{w}_o = \mathbf{R}^{-1}\mathbf{p},$$

being $\mathbf{R} = \mathrm{E}\{\mathbf{r}(n)\mathbf{r}^T(n)\}$ the autocorrelation matrix of the input signal of the equalizer and $\mathbf{p} = \mathrm{E}\{s(n-\Delta)\mathbf{r}(n)\}$, the cross-correlation vector between the input signal and the sequence $s(n-\Delta)$. The Wiener solution is known as optimal linear solution and depends on the delay Δ. Since most adaptive filters converge in the mean to the Wiener solution, it is considered as a benchmark for the cNLMS algorithm. The EMSE measures how much $\mathrm{E}\{\hat{J}(n)\}$ exceeds its minimum value due to adaptation. If the algorithm found the Wiener solution $\mathbf{w}_o$ at each time instant, the EMSE would be zero. Since the actual filter coefficients are never exactly equal to the optimum values, the EMSE measures the effect of this difference on the error variance [17,18].

Another performance measure considered in this paper is the bit error rate (BER) [16]. BER curves were estimated after the convergence of cNLMS and counting the number of errors when comparing $m(n-\Delta)$ with the sequence obtained at the output of a decision device applied to $\hat{m}(n)$. We disregarded 3×10^5 bits due to the initial convergence and used 10^6 bits in to computation of the BER. In this case, the BER obtained with the Wiener solution is considered as benchmark for the proposed scheme.

We first assume that $m(n) \equiv 1$ and, consequently, $s(n) = x_1(n)$. In this case, the output of the communication channel is assumed to be related to its input by the following difference equation

$$r(n) = s(n) - 0.6r(n-1),$$

which corresponds to the following transfer function

$$H_1(z) = \frac{1}{1 + 0.6z^{-1}}.$$

Since $H_1(z)$ is an infinite impulse response (IIR) channel and the equalizer is assumed to be a finite impulse response (FIR) filter, the perfect equalization is possible in the absence of noise. In this simple case,

$$\mathbf{w}_o = [1 \quad 0.6]^T. \tag{22}$$

Although there is no transmission of information between master and slave in this situation, this simulation shows that the equalizer plays an essential role to enable the synchronization of the map as we shall see next.

The effect of the channel $H_1(z)$ can be observed by comparing the reconstructed attractors, using $s(n)$ and $r(n)$. Due to the channel effect, the dynamical characteristics of the signal $s(n) = x_1(n)$ are lost, as observed by comparing the attractors of Figs. 3(a) and 3(b). In Fig. 3(c), it is possible to notice that the equalizer is able to eliminate the channel effect, recovering an attractor similar to the original one.

The sequence $\hat{m}(n)$ estimated by the cNLMS equalizer is shown in Fig. 4(b). The average of the two coefficients and the EMSE along the iterations, estimated by an ensemble-average of 1000 runs, are shown respectively in Figs. 4(c) and (e). We can observe that cNLMS coefficients approach to $\mathbf{w}_o$ of (22), as shown by the dashed lines in Fig. 4(c). Therefore, the equalizer is working as expected since this solution mitigates the intersymbol interference, enabling the synchronization of the Hénon map, which can be confirmed by means of Fig. 4(d), since for $n > 2000$ the graphic of $x_1(n)$ vs. $\hat{x}_1(n)$ becomes close to a line (blue dots in the figure). There is no synchronization in the case with no equalizer as shown in Fig. 4(a).

In the following simulations, we assume the transmission of a binary equiprobable random sequence $m(n) \in \{-1, 1\}$. We consider

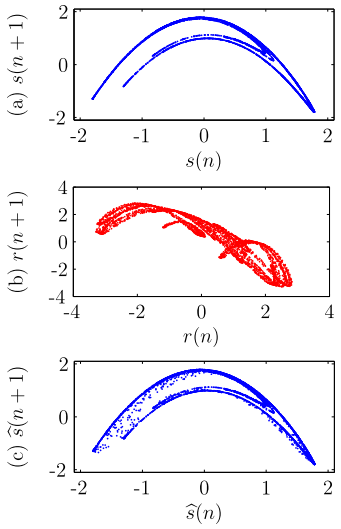

Fig. 3. Reconstructed attractor using the: (a) transmitted, (b) received and (c) recovered with cNLMS signals in the case $m(n) \equiv 1$; $M = 2$; $\Delta = 0$; $H_1(z)$.

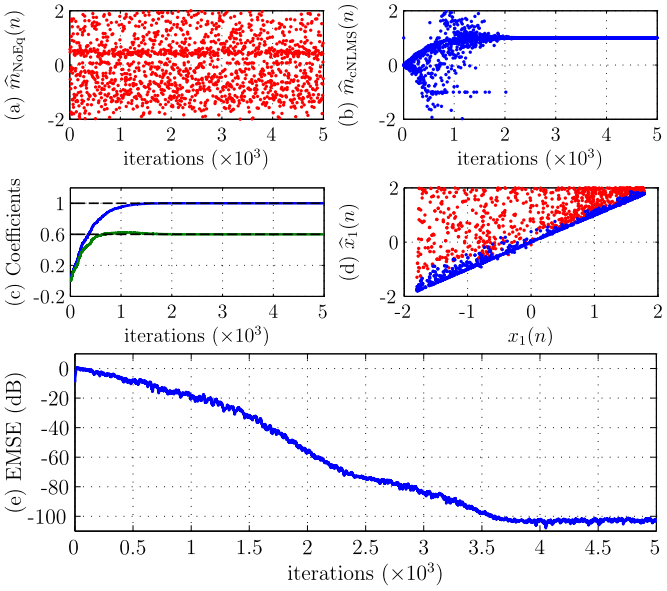

Fig. 4. Recovered sequence with (a) no equalizer and (b) one run of cNLMS ($\mu = 0.005$, $\delta = 10^{-5}$, $\varepsilon = 0.1$); (c) average of the coefficients of cNLMS and Wiener solution (dashed lines); (d) $x_1(n)$ *vs.* $\hat{x}_1(n)$: red dots for $0 < n \leq 2000$ and blue dots for $n > 2000$ (e) estimated EMSE; average of 1000 runs; $M = 2$; $\Delta = 0$; $H_1(z)$. (For interpretation of the references to color in this figure legend, the reader is referred to the web version of this article.)

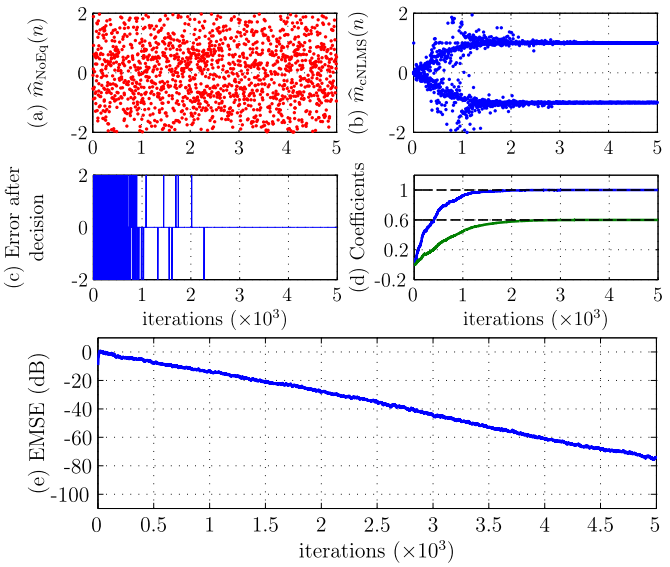

Fig. 5. Recovered sequence with (a) no equalizer and (b) cNLMS ($\mu = 0.005$, $\delta = 10^{-5}$, $\varepsilon = 0.1$); (c) error after decision; (d) average of the coefficients of cNLMS and Wiener solution (dashed lines); (e) estimated EMSE; average of 1000 runs; $M = 2$; $\Delta = 0$; $H_1(z)$.

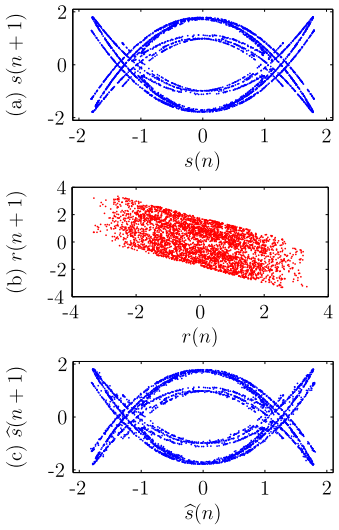

Fig. 6. Reconstructed attractor using the: (a) transmitted, (b) received and (c) recovered with cNLMS signals in the case of $m(n)$ binary equiprobable random sequence (parameters as in Fig. 5).

again Channel $H_1(z)$ with $\Delta = 0$ and absence of noise. The sequence estimated via the cNLMS equalizer and the error after the decision device (both for one realization) are shown in Figs. 5(b) and (c). The average of the two coefficients and the EMSE along the iterations, estimated by an ensemble-average of 1000 runs, are shown respectively in Figs. 5(d) and (e). Again, cNLMS approaches to $\mathbf{w}_o$ of (22) and the equalizer recovers properly the transmitted sequence, which can be confirmed through the errors after the decision device shown in Fig. 5(c). The communication is completely lost in the case with no equalizer as shown in Fig. 5(a).

The effect of the communication channel can also be observed by means of the reconstructed attractors using the transmitted and received signals. They are shown in Figs. 6(a) and 6(b). Due to the channel effect, the dynamical characteristics of the transmitted signal are lost, as observed in Fig. 6(b). In Fig. 6(c), it is possible to notice that the equalizer is able to eliminate the channel effect, recovering again an attractor similar to the original one.

Next, we verify the behavior of the equalizer in case of an abrupt variation in the channel. For this, we consider the following noiseless scenario: initially, $s(n)$ is transmitted through the real part of the telephonic channel of [29], so that $r(n)$ is given by

$$\begin{aligned} r(n) = {} & -0.005s(n) + 0.009s(n-1) - 0.024s(n-2) \\ & + 0.850s(n-3) - 0.218s(n-4) + 0.050s(n-5) \\ & - 0.016s(n-6). \end{aligned}$$

Then, at $n = 5 \times 10^3$, this channel is abruptly changed to the imaginary part of the same telephonic channel, i.e.,

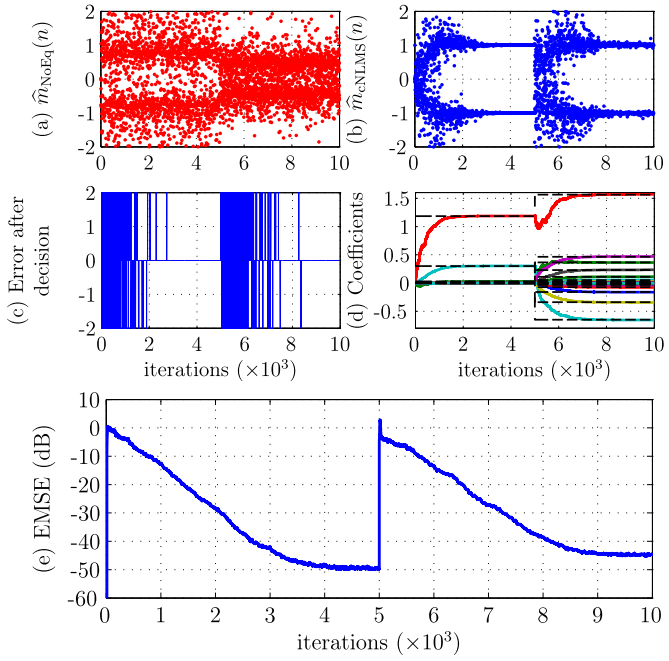

Fig. 7. Recovered sequence with (a) no equalizer and (b) cNLMS ($\mu = 0.2$, $\delta = 10^{-5}$, $\varepsilon = 0.1$); (c) error after decision; (d) average of the coefficients of cNLMS and Wiener solution (dashed lines); (e) estimated EMSE; average of 1000 runs; $M = 25$; $\Delta = 12$; abrupt time-varying channel scenario.

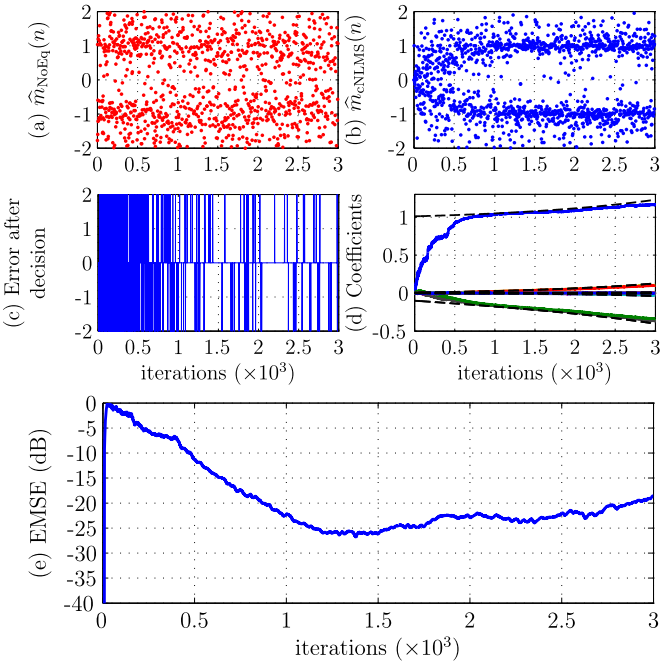

Fig. 8. Recovered sequence with (a) no equalizer and (b) cNLMS ($\mu = 0.2$, $\delta = 10^{-5}$, $\varepsilon = 0.1$); (c) error after decision; (d) average of the coefficients of cNLMS and Wiener solution (dashed lines); (e) estimated EMSE; average of 1000 runs; $M = 15$; $\Delta = 8$; smooth time-varying channel scenario.

$$r(n) = -0.004s(n) + 0.030s(n-1) - 0.104s(n-2) + 0.520s(n-3) + 0.273s(n-4) - 0.074s(n-5) + 0.020s(n-6).$$

For both channels, we assumed an equalizer with $M = 25$ coefficients and a delay of $\Delta = 12$ samples.

The results for this scenario are shown in Fig. 7. As it can be noticed, cNLMS converges to the Wiener solution [18], whose coefficients are shown as dashed lines in Fig. 7(d). It is important to notice that cNLMS is able to track the abrupt variation in the channel, achieving the steady-state again. The equalizer plays an important role to mitigate the intersymbol interference since the performance of the system without equalizer is much worse as observed in Fig. 7(a).

To verify the behavior of the equalizer with a time-varying channel, we considered the transmission of $s(n)$ through the noiseless channel, given by

$$r(n) = h_0(n)s(n) + s(n-1) + h_0(n)s(n-2), \tag{23}$$

in which $h_0(n)$ varies linearly from 0.1 to 0.3 at $n = 0$ and $n = 3 \times 10^3$, respectively. The results for this scenario are shown in Fig. 8. As it can be noticed, the equalizer is able to adapt as the channel varies, obtaining a good estimate of the instantaneous Wiener solution, shown by the dashed lines of Fig. 8(d).

To show the sensitivity of chaotic synchronization to the intersymbol interference (ISI), we obtain BER curves of the system for the channel given by (23) in the absence of noise with $M = 21$ and $\Delta = 11$. They are shown in Fig. 9. It is important to remark that in the case with no equalizer, the delay is due only to the channel. Therefore, we compared the recovered sequence with $m(n - \Delta)$, assuming $\Delta = 1$ in this case. The smaller the value of h_0 the lower the intersymbol interference introduced by the channel. We can observe that cNLMS eliminates approximately the channel effects, achieving a *quasi*-perfect equalization (BER $< 10^{-5}$) for $0 \leq h_0 \leq 0.15$, whereas the Wiener solution provides a *quasi*-perfect equalization for $0 \leq h_0 \leq 0.25$. The distance between cNLMS and Wiener is due to the step size ($\mu = 0.05$) considered in the simulations. It is well known that there is a tradeoff in all adaptive algorithms, which states that the smaller the step size, the smaller the steady-state EMSE (and BER), and consequently the closer the algorithm to the Wiener solution [17,18]. However, a too small step-size causes a low convergence and the algorithm may not be able to track the variations in the channel. Both solutions outperform the case with no equalizer for $0 < h_0 < 0.5$. In the case of $h_0 = 0$, we have the ideal channel and the equalizer is not necessary. Note that a minor channel imperfection (e.g., $h_0 = 0.05$) is enough to completely lose the transmitted message and the equalizer is essential to permit communication. In the case of $h_0 = 0.5$, the channel presents a deep spectral null and instead of a linear transversal equalizer, we should use a decision feedback equalizer to eliminate the channel effects [16,18].

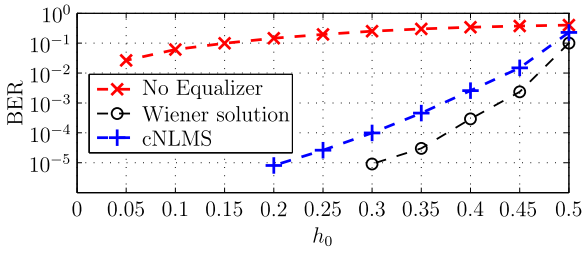

Fig. 9. Bit error rate for the channel (23) as function of h_0 in the absence of noise; cNLMS ($\tilde{\mu} = 0.05$, $\delta = 10^{-5}$, $\varepsilon = 0.1$).

To show also the sensitivity of chaotic synchronization to noise, we added white Gaussian noise to the signal at the output of the channel (23) in order to obtain a signal-to-noise ratio (SNR) of 60 dB. The BER curves for this case are shown in Fig. 10. Since the equalizer only tries to eliminate the ISI, the bit error rates are

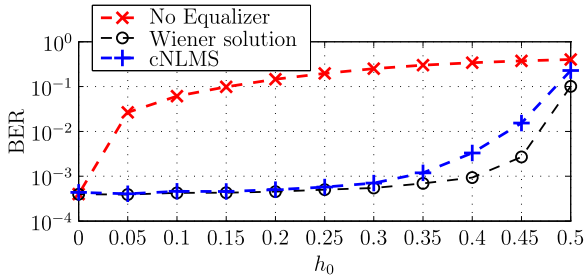

Fig. 10. Bit error rate for the channel (23) as function of h_0 with SNR = 60 dB; cNLMS ($\tilde{\mu} = 0.05$, $\delta = 10^{-5}$, $\varepsilon = 0.1$).

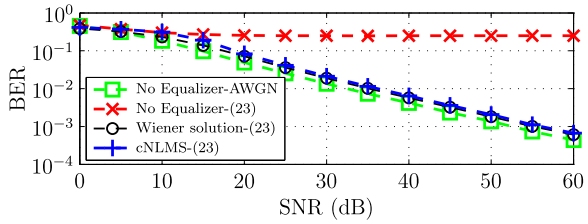

Fig. 11. Bit error rate for the non-dispersive AWGN channel and for the channel (23) with $h_0 = 0.25$ as a function of SNR; cNLMS ($\tilde{\mu} = 0.05$, $\delta = 10^{-5}$, $\varepsilon = 0.1$).

higher that those of Fig. 9, mainly when the ISI is low. Even for the ideal channel ($h_0 = 0$), the perfect recovery of the message is not possible since we have a BER of approximately 8×10^{-4}. Assuming again the channel (23) with $h_0(n) = 0.25$, we obtain BER curves as a function of SNR as shown in Fig. 11. For comparison, we also include the BER curve for the non-dispersive AWGN channel, obtained with the system of Fig. 1 without equalizer. This BER curve works as a benchmark for the equalization in a noisy and dispersive environment. The closer the BER obtained in a dispersive and noisy channel to the BER of the AWGN channel, the more efficient in terms of mitigation of ISI the equalizer is. We can observe that the BER obtained with the cNLMS algorithm is close to that of the Wiener solution, and both are slightly outperformed by the AWGN case. Again, the absence of the equalizer in a dispersive channel leads to prohibitive error rates. It is important to emphasize that to permit chaotic communications using the system of Fig. 1 in the presence of noise, the transmitter should encode the signal $s(n)$ using an error-correcting code prior to transmission [16].

6. Conclusion

In this paper, we proposed a supervised equalization scheme based on the NLMS algorithm for a master–slave synchronization scheme using maps. Simulations of different scenarios show that the proposed algorithm can successfully permit chaotic synchronization for non-ideal channels. For low signal-to-noise ratios, it is essential to include error-correcting codes in the transmitter, since the equalizer only deals with intersymbol interference. Although we considered the Hénon map in the simulations, the cNLMS algorithm can be modified to be used with other chaotic maps, e.g., the Ikeda map [24]. As an example of application, the proposed scheme was used to recover a binary polar sequence in a chaos-based digital communication system.

Acknowledgments

This work was partly supported by FAPESP under Grants 2014/04864-2 and 2012/24835-1 and by CNPq under Grants 303926/2010-4 and 302423/2011-7.

References

[1] L.M. Pecora, T.L. Carroll, Synchronization in chaotic systems, Phys. Rev. Lett. 64 (8) (1990) 821–824.
[2] K.M. Cuomo, A.V. Oppenheim, Circuit implementation of synchronized chaos with applications to communications, Phys. Rev. Lett. 71 (1) (1993) 65–68.
[3] C.W. Wu, L.O. Chua, A simple way to synchronize chaotic systems with applications to secure communication systems, Int. J. Bifurc. Chaos 3 (6) (1993) 1619–1627.
[4] A. Argyris, D. Syvridis, L. Larger, V. Annovazzi-Lodi, P. Colet, I. Fischer, J. Garcia-Ojalvo, C.R. Mirasso, L. Pesquera, K.A. Shore, Chaos-based communications at high bit rates using commercial fibre-optic links, Nature 438 (7066) (2005) 343–346.
[5] M. Eisencraft, R. Attux, R. Suyama (Eds.), Chaotic Signals in Digital Communications, CRC Press, Inc., 2013.
[6] K.T. Alligood, T. Sauer, J.A. Yorke, Chaos: An Introduction to Dynamical Systems, Textbooks in Mathematical Sciences, Springer-Verlag, New York, 1997.
[7] M.P. Kennedy, G. Setti, R. Rovatti (Eds.), Chaotic Electronics in Telecommunications, CRC Press, Inc., Boca Raton, FL, USA, 2000.
[8] F.C.M. Lau, C.K. Tse, Chaos-Based Digital Communication Systems, Springer, Berlin, 2003.
[9] W. Tam, F. Lau, C. Tse, Digital Communications with Chaos: Multiple Access Techniques and Performance, Elsevier, 2007.
[10] M. Feki, B. Robert, G. Gelle, M. Colas, Secure digital communication using discrete-time chaos synchronization, Chaos Solitons Fractals 18 (4) (2003) 881–890.
[11] A. Uchida, Optical Communication with Chaotic Lasers: Applications of Nonlinear Dynamics and Synchronization, Wiley-VCH, Singapore, 2012.
[12] C. Williams, Chaotic communications over radio channels, IEEE Trans. Circuits Syst. I 48 (12) (2001) 1394–1404.
[13] M. Eisencraft, R.D. Fanganiello, J.M.V. Grzybowski, D.C. Soriano, R.F. Attux, A.M. Batista, E.E.N. Macau, L.H.A. Monteiro, J.M.T. Romano, R. Suyama, T. Yoneyama, Chaos-based communication systems in non-ideal channels, Commun. Nonlinear Sci. Numer. Simul. 17 (12) (2012) 4707–4718.
[14] F.O. Souza, R.M. Palhares, E.M.A.M. Mendes, L.A.B. Torres, Synchronizing continuous time chaotic systems over nondeterministic networks with packet dropouts, Int. J. Bifurc. Chaos 22 (12) (2012), http://dx.doi.org/10.1142/S0218127412503002.
[15] H.-P. Ren, M.S. Baptista, C. Grebogi, Wireless communication with chaos, Phys. Rev. Lett. 110 (2013), http://dx.doi.org/10.1103/PhysRevLett.110.184101.
[16] S. Haykin, Communication Systems, 4th edition, Wiley, New York, 2000.
[17] S. Haykin, Adaptive Filter Theory, 4th edition, Prentice Hall, Upper Saddle River, 2002.
[18] A.H. Sayed, Adaptive Filters, John Wiley & Sons, NJ, 2008.
[19] H. Leung, System identification using chaos with application to equalization of a chaotic modulation system, IEEE Trans. Circuits Syst. I 45 (3) (1998) 314–320.
[20] M. Ciftci, D. Williams, A novel channel equalizer for chaotic digital communications systems, in: Proc. IEEE Int. Conf. Acoustics, Speech, and Signal Process., Phoenix, AZ, 1999, pp. 1301–1304.
[21] Z. Zhu, H. Leung, Adaptive blind equalization for chaotic communication systems using extended-Kalman filter, IEEE Trans. Circuits Syst. I 48 (8) (2001) 979–989.
[22] J. Feng, C.K. Tse, F.C.M. Lau, Reconstruction of chaotic signals with application to channel equalization in chaos-based communication systems, Int. J. Commun. Syst. 17 (2004) 217–232.
[23] C. Vural, G. Çetinel, Blind equalization of single-input single-output fir channels for chaotic communication systems, Digit. Signal Process. 20 (1) (2010) 201–211.
[24] R. Candido, M. Eisencraft, M.T.M. Silva, Channel equalization for synchronization of Ikeda maps, in: Proc. of the 21st European Signal Processing Conference (EUSIPCO'2013), Marrakesh, Marocco, 2013.
[25] L.M. Pecora, T.L. Carroll, G.A. Johnson, D.J. Mar, J.F. Heagy, Fundamentals of synchronization in chaotic systems, concepts, and applications, Chaos, Interdiscip. J. Nonlinear Sci. 7 (4) (1997) 520–543.
[26] M. Hénon, A two-dimensional mapping with a strange attractor, Commun. Math. Phys. 50 (1976) 69–77.
[27] M. Eisencraft, R.D. Fanganiello, L.A. Baccalá, Synchronization of discrete-time chaotic systems in bandlimited channels, Math. Probl. Eng. (2009), http://dx.doi.org/10.1155/2009/207971.
[28] W.A. Sethares, Adaptive algorithms with nonlinear data and error functions, IEEE Trans. Signal Process. 40 (9) (1992) 2199–2206.
[29] G. Picchi, G. Prati, Blind equalization and carrier recovery using a "stop-and-go" decision-directed algorithm, IEEE Trans. Commun. COM-35 (1987) 877–887.

Renato Candido was born in São Paulo, Brazil, in 1982. He received the B.S. degree in Electronics Engineering from Mackenzie Presbyterian University, São Paulo, Brazil, in 2007 and the M.S. degree in Electrical En-

gineering from Escola Politécnica, University of São Paulo, Brazil, in 2009. He is currently working towards the Ph.D. degree in Electrical Engineering at the same university. His research interests include Signal Processing and Adaptive Filtering.

Marcio Eisencraft was born in São Paulo, Brazil. He received the B.S., M.S. and Ph.D. degrees in Electrical Engineering from Escola Politénica, University of São Paulo, São Paulo, Brazil, in 1998, 2001 and 2006, respectively. From February 2001 to February 2010 he was an Assistant Professor at Mackenzie Presbyterian University, São Paulo. From March 2010 to July 2013 he was an Assistant Professor at Universidade Federal do ABC, Santo André, Brazil. Since August 2013, he is an Assistant Professor at the Department of Telecommunications and Control Engineering at Escola Politécnica, University of São Paulo. His research interests include Digital Communications, Signal Processing, and Dynamical Systems.

Magno T.M. Silva was born in São Sebastião do Paraíso, Brazil. He received the B.S. degree in 1998, the M.S. degree in 2001, and the Ph.D. degree in 2005, all in Electrical Engineering from Escola Politécnica, University of São Paulo, São Paulo, Brazil. From February 2005 to July 2006 he was an Assistant Professor at Mackenzie Presbyterian University, São Paulo. Since August 2006, he has been with the Department of Electronic Systems Engineering at Escola Politécnica, University of São Paulo, where he is currently an Associate Professor. From January to July 2012, he worked as a Postdoctoral Researcher at the Universidad Carlos III de Madrid, Leganés, Spain. His research interests include Signal Processing and Adaptive Filtering.